

Temperature dependence of the vibrational modes of molybdenum

J. Zarestky, C. Stassis, B. N. Harmon, K.-M. Ho, and C. L. Fu
 Ames Laboratory—U.S. Department of Energy, Iowa State University, Ames, Iowa 50011
 and Department of Physics, Iowa State University, Ames, Iowa 50011
 (Received 7 December 1982; revised manuscript received 18 March 1983)

Inelastic neutron scattering techniques have been used to study the temperature dependence of the phonon dispersion curves of bcc Mo. We find that, with increasing temperature, the largest relative decrease in phonon frequencies ($\sim 12\%$) occurs for the $L[\xi\xi\xi]$ branch in the vicinity of $\xi = \frac{2}{3}$. The phonon frequencies in the vicinity of the H point in the Brillouin zone, on the other hand, increase slightly with increasing temperature. As a result, at high temperatures, the anomalous drop in the phonon frequencies at H decreases in magnitude and the $L[\xi\xi\xi]$ branch develops a dip at $\xi = \frac{2}{3}$. The experimental results also indicate that the phonon anomaly in the vicinity of point N is less pronounced at high temperatures. For the purpose of comparison with the experimental results, we have performed first-principle "frozen-phonon" calculations for the longitudinal-phonon frequencies of Mo at the $(\frac{2}{3}, \frac{2}{3}, \frac{2}{3})$ and H points of the Brillouin zone. The results show that thermal expansion and anharmonicity can account for the temperature dependence of the $(\frac{2}{3}, \frac{2}{3}, \frac{2}{3})$ longitudinal-phonon frequency. For the H phonon, on the other hand, the thermal expansion and anharmonicity terms cannot account for the observed frequency shift and we suggest that the contributions arising from the electron-phonon renormalization and the thermal disorder of the lattice must be included.

I. INTRODUCTION

The transition metals molybdenum, tungsten, and chromium are all body-centered-cubic (bcc) with one atom per primitive cell, and they possess similar electronic properties. As a result, the dispersion curves of these metals¹⁻⁷ are quite similar and exhibit anomalies near the symmetry points N and H , which have been associated with the nesting properties of the Fermi surface. The most outstanding feature¹⁻⁷ of the dispersion curves of these metals is, however, the absence of any appreciable dip in the phonon frequencies of the $L[\xi\xi\xi]$ branch for propagation vectors in the vicinity of $\bar{q} = \frac{2}{3}[111]$.

For a monatomic bcc structure one would have expected, independently of any particular model, a relative decrease of the phonon frequencies of the $L[\xi\xi\xi]$ branch in the vicinity of $\bar{q} = \frac{2}{3}[111]$, since for this vibrational mode the nearest-neighbor distance between atoms along the $[111]$ direction remains unchanged, and therefore, the corresponding restoring force vanishes. It has been shown that this effect is characteristic of the dispersion curves of the purely ionic bcc lattice,⁸ and it has been observed in the measured dispersion curves of a large number of monatomic bcc metals. It is, therefore, natural to assume that the dip in the phonon frequencies of the $L[\xi\xi\xi]$ branch at $\bar{q} = \frac{2}{3}[111]$ is a geometrical property of the bcc lattice, an assumption supported by recent theoretical considerations.⁹ In view of the above discussion, it is tempting to assume that the absence of this effect in Mo, Cr, and W is due to some special aspect of the electronic structure of these metals. To investigate this point and to assess the detailed temperature dependence of the anomalies at points N and H , we performed a systematic study of the dispersion curves of Mo as a function of temperature. In this paper we present the experimental data and the results of first-principles "frozen-phonon" calcu-

lations which were used in the interpretation of the experimental results.

II. EXPERIMENTAL DETAILS

The measurements were performed on a large single crystal ($\sim 5 \text{ cm}^3$) of molybdenum grown at the Materials Preparation Center of the Ames Laboratory. The frequencies of the vibrational modes, with wave vectors along the $[00\xi]$, $[\xi\xi 0]$, and $[\xi\xi\xi]$ symmetry directions, were measured at 295 and 1203 K. The frequencies of a selected number of phonons were also measured at 10.5 K. The high-temperature measurements were performed in a vacuum neutron-diffraction furnace, and the low-temperature measurements in a standard closed-cycle He refrigerator.

The measurements were performed on a triple-axis spectrometer at the Oak Ridge Research Reactor (ORR) of the Oak Ridge National Laboratory. All data were collected using the constant \bar{Q} (where \bar{Q} is the neutron scattering

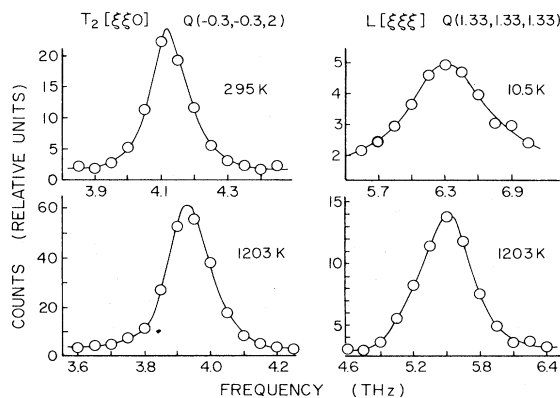


FIG. 1. Some typical neutron groups.

TABLE I. Measured phonon frequencies (THz) at 295, 1203, and 10.5 K, of bcc Mo.

	ξ 295 K	$\nu \pm \Delta\nu$ 1203 K	10.5 K		ξ 295 K	$\nu \pm \Delta\nu$ 1203 K	10.5 K
		T[00 ξ]				L[00 ξ]	
0.15	1.53±0.02	1.48±0.02	1.60±0.03	0.20	4.13±0.06	3.82±0.05	4.13±0.06
0.40	3.96±0.02	3.83±0.02	4.08±0.02	0.40	6.73±0.05	6.37±0.05	6.93±0.06
0.50	4.61±0.02	4.49±0.03		0.60	7.70±0.06	7.13±0.06	
0.60	5.19±0.05	5.10±0.03		0.80	7.18±0.08	6.72±0.08	7.29±0.08
0.70		5.54±0.04		0.85	6.87±0.10	6.61±0.08	7.00±0.08
0.75	5.77±0.04	5.67±0.06		0.90	6.30±0.11	6.23±0.10	6.55±0.10
0.80	5.93±0.05	5.72±0.06		0.95	5.66±0.15	5.93±0.10	
0.85	6.09±0.08	5.73±0.08		0.98	5.59±0.08	5.85±0.06	
0.90	5.91±0.08	5.76±0.08	5.93±0.06	1.00	5.53±0.05	5.73±0.06	5.51±0.05
0.95	5.61±0.07	5.74±0.06	5.58±0.06				
0.98	5.59±0.06	5.74±0.05					
1.00	5.53±0.05	5.73±0.06	5.51±0.05				
		T ₁ [$\xi\xi0$]				T ₂ [$\xi\xi0$]	
				0.10	1.42±0.03	1.36±0.03	1.46±0.02
				0.20	2.84±0.04	2.74±0.03	2.90±0.02
				0.30	4.12±0.02	3.94±0.02	
0.10	1.69±0.05	1.54±0.02		0.325	4.35±0.02		
0.15	2.47±0.03	2.25±0.03		0.35	4.60±0.02	4.38±0.03	
0.20		2.96±0.03		0.375	4.72±0.03		
0.25	3.98±0.02	3.57±0.02		0.40	4.85±0.03	4.64±0.04	4.86±0.05
0.30		4.11±0.03		0.425	4.77±0.04		
0.35	5.07±0.02	4.57±0.03		0.45	4.74±0.03	4.64±0.04	4.75±0.06
0.40		4.93±0.05		0.475	4.58±0.06		
0.45		5.17±0.05		0.50	4.59±0.05	4.60±0.07	4.59±0.07
0.50		5.31±0.07					
		L[$\xi\xi0$]				L[$\xi\xi\xi$]	
0.10	2.94±0.05	2.80±0.04	2.87±0.04	0.10	3.45±0.06	3.30±0.06	
0.20	5.20±0.03	5.02±0.03	5.22±0.04	0.20	5.81±0.07	5.59±0.05	5.78±0.08
0.30	6.75±0.03	6.46±0.04		0.30	6.65±0.08	6.43±0.08	
0.40	7.67±0.08	7.29±0.05		0.40	7.10±0.07	6.72±0.07	
0.50	8.24±0.07	7.61±0.10	8.35±0.07	0.50	6.46±0.06	6.12±0.05	
				0.55	6.28±0.05	5.81±0.05	
				0.60	6.24±0.06	5.65±0.06	
				0.67	6.14±0.05	5.49±0.05	6.31±0.04
				0.70	6.16±0.06	5.45±0.05	
0.20	3.89±0.04	3.51±0.03	4.00±0.03	0.75	6.23±0.05	5.51±0.06	
0.30	5.36±0.03	4.90±0.02		0.80	6.10±0.05	5.59±0.06	
0.40	6.19±0.04	5.72±0.05		0.85	6.18±0.05	5.72±0.06	
0.50	6.46±0.06	6.12±0.05		0.90	6.24±0.08	5.93±0.06	
0.60	6.79±0.06	6.48±0.08		0.93	6.30±0.04	6.01±0.05	
0.70	7.02±0.06	6.68±0.06	7.20±0.10	0.96	6.10±0.05	5.87±0.05	
0.80	6.82±0.04	6.48±0.05		0.98	5.73±0.04	5.73±0.05	5.72±0.05
0.90	6.10±0.04	5.95±0.08		0.99	5.55±0.04	5.68±0.05	5.55±0.05
0.95	5.68±0.05	5.78±0.05		1.00	5.53±0.05	5.73±0.06	5.51±0.05
0.98	5.55±0.08	5.76±0.05					

vector) mode of operation and a fixed scattered neutron energy of 3.6 THz. Pyrolytic graphite, reflecting from the (002) planes, was used as both monochromator and analyzer, and a pyrolytic graphite filter was placed in the scattered beam to attenuate higher-order contaminations. The collimation of the neutron beam before and after the sample was 40 min of arc. The neutron groups at various temperatures were all obtained under identical experimental configurations.

The phonon frequencies were obtained by determining the centroids of the measured neutron groups. Some typical neutron groups are shown in Fig. 1. The frequencies

of a large number of vibrational modes were determined by measurements around equivalent reciprocal-lattice points; in all cases the frequencies were found to agree to within experimental precision and their average was adopted. Particular care was taken to avoid systematic errors in assessing the frequency shifts as a function of temperature. The room-temperature data were first obtained with the crystal mounted in the diffraction furnace, next the high-temperature data were taken under identical experimental configurations, and then the furnace was turned off and a large number of phonon frequencies were checked after the crystal was cooled to room temperature.

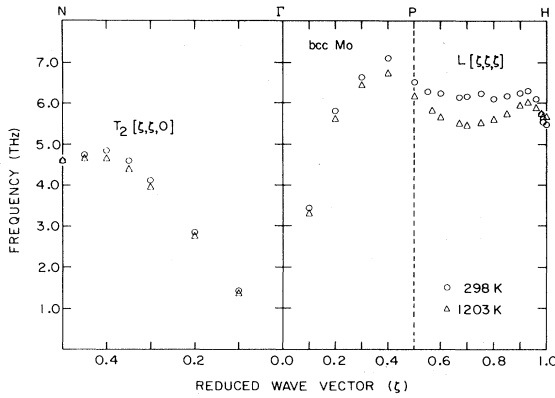


FIG. 2. Comparison of the room-temperature and 1203-K dispersion curves of bcc Mo.

A similar procedure was followed for the low-temperature measurements, which were performed with the crystal mounted in a standard refrigerator.

III. EXPERIMENTAL RESULTS AND DISCUSSION

The measured phonon frequencies are listed in Table I. The room-temperature and 1203-K dispersion curves are compared in Fig. 2, and the main results are illustrated in Fig. 3. The room-temperature data are in excellent agreement with the results obtained by Woods and Chen,⁷ and by Powell *et al.*² in their detailed studies of the room-temperature dispersion curves of molybdenum. To within the resolution of the present measurements, we did not observe any appreciable broadening of the measured neutron groups with increasing temperature (see Fig. 1). Also, our results for the temperature dependence of the L[00ξ] branch are consistent with the measurements at 88 K obtained for this branch by Buyers, Powell, and Woods.¹⁰

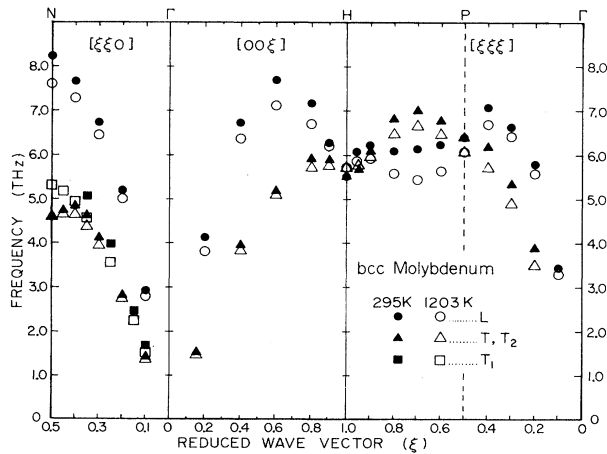


FIG. 3. Measured phonon frequencies at 295 and 1203 K for the L[ξξξ] and T₂[ξξ0] branches of bcc Mo. For clarity, the 10.5 K data were omitted (see Table I).

It can be seen (Table I and Figs. 2 and 3) that all phonon frequencies, except in the vicinity of the symmetry points *H* and *N*, decrease with increasing temperature and that the largest relative decrease ($\sim 12\%$) occurs for the L[ξξξ] branch in the vicinity of $\vec{q} = \frac{2}{3}[111]$. The phonon frequencies near the point *H*, on the other hand, increase slightly with increasing temperature (Table I and Figs. 2 and 3). As a result, at high temperatures the anomalous drop in the phonon frequencies at point *H* decreases in magnitude and the L[ξξξ] branch develops a dip in the vicinity of $\vec{q} = \frac{2}{3}[111]$. Thus with increasing temperature, the shape of the L[ξξξ] branch of Mo approaches that of a typical monatomic bcc metal. The effect of changes in temperature on the phonon frequencies of the T₂[ξξ0] branch are not as dramatic as for the L[ξξξ] branch. The experimental results, however, do indicate (Fig. 3) that the anomalous features of this branch are also less pronounced at high temperatures.

Theoretical studies of the temperature dependence of the phonon frequencies of transition metals and compounds have trailed experiment, except for a few phenomenological studies of soft-mode behavior in compounds. This is true for the whole field of transition-metal lattice dynamics where until recently the difficulty of accurately treating the electron-phonon interaction in these metals prevented a close comparison between theory and experiment, and led to the use of elaborate schemes for fitting the experimental data with a large number of physically questionable parameters. A significant theoretical step was made a few years ago by Varma and Weber who used a tight-binding method for evaluating the electron-phonon matrix elements and calculated the phonon dispersion curves for Nb, Mo, and Nb-Mo alloys.¹¹ They were successful in demonstrating that the sharp phonon anomalies found in many transition metals are related to the electronic structure near the Fermi surface. Although Varma and Weber applied their method to molybdenum, their results are not so useful for the present study since their method employs a few adjustable parameters to model short-range interactions and is restricted to harmonic forces. Rather than extend the Varma and Weber techniques to third-order terms, a newly developed frozen-phonon method was used which allows the accurate calculation of phonon frequencies entirely from first principles,^{12,13} and can provide information about anharmonic effects. For computational reasons, the frozen-phonon method can only be efficiently employed for a restricted number of wave vectors, and in this study the calculations are limited to the most interesting phonons at $\vec{q} = (\frac{2}{3}, \frac{2}{3}, \frac{2}{3})$ and the *H* point.

In first-principles frozen-phonon calculations, the lattice is subjected to a static distortion corresponding to a particular phonon mode, and the total energy of the crystal as a function of displacement is obtained from self-consistent band-structure calculations. The phonon frequency is then determined from the curvature of the calculated energy-displacement curve. An account of these calculations has been given elsewhere,¹² and further details will be published in a future paper.¹³ In the following, we present a summary of the most pertinent results. The calculated values for the frequencies of the $(\frac{2}{3}, \frac{2}{3}, \frac{2}{3})$ and *H* points at 0 K, are 6.0 and 5.1 THz, respectively, in fair

agreement with the low-temperature measurements (6.31 ± 0.04 and 5.54 ± 0.06 THz, respectively). The calculations show that the drop in frequency at H is due to the large band splitting at the Fermi level occurring for displacements corresponding to this phonon, a conclusion which is in agreement with calculations by Varma and Weber.¹³ The absence of a dip in frequency at $(\frac{2}{3}, \frac{2}{3}, \frac{2}{3})$ of the $L[\xi\xi\xi]$ branch, on the other hand, cannot be associated with features of the bands at the Fermi level. To assess the origin of this effect, the contributions of the different electronic states to the interatomic forces have been determined by use of the Hellman-Feynman theorem. It is found that the increase in frequency above the value expected for a typical monatomic bcc metal is due to bond-bending forces arising from the directional bonding developed within the d bands. The $(\frac{2}{3}, \frac{2}{3}, \frac{2}{3})$ longitudinal phonon is unique in that the interatomic distances along the $[111]$ direction are preserved as the lattice is distorted. Thus the atomic displacements for this mode can be viewed as a shearing motion between chains of atoms along the $[111]$ direction. In most monoatomic bcc metals (unlike Mo), a dip in frequency at $(\frac{2}{3}, \frac{2}{3}, \frac{2}{3})$ occurs for the longitudinal branch. Since the dominant intrachain restoring forces go to zero at $(\frac{2}{3}, \frac{2}{3}, \frac{2}{3})$, this indicates that the bond-bending forces are weak. At high temperatures in Mo, a dip begins to appear also, and it suggests that the directional d bonding is reduced by the increased thermal disorder.

To study the origin of the temperature dependence of the phonon frequencies, the effect of the thermal expansion of the lattice as well as the anharmonic contribution arising from the nonparabolic shape of the calculated potential wells were considered. The effect of the thermal expansion of the lattice can be obtained accurately, since it involves the difference of two values calculated in an identical manner. We evaluated the energy-displacement potential wells for the expanded lattice at 1000 K and found that, as a result of the thermal expansion, the frequency of the $(\frac{2}{3}, \frac{2}{3}, \frac{2}{3})$ longitudinal phonon is decreased, at 1000 K, by 0.11 ± 0.02 THz. To estimate the effect of anharmonicity the calculated energy-displacement curve was treated as an atomic potential well, and the change in interlevel spacing when the energy per atom is increased by kT was calculated. This procedure, although not rigorously correct, can be shown to provide a reasonable approximation to the results of self-consistent phonon theories¹⁴ if the anharmonic forces are weak and of short range. For

the $(\frac{2}{3}, \frac{2}{3}, \frac{2}{3})$ longitudinal phonon, this leads to a decrease in frequency of approximately 0.4 THz at 1000 K. Thus for this phonon, the estimated net decrease in frequency is 0.5 THz at 1000 K. In view of the uncertainties involved in the evaluation of the anharmonic contribution, this result is in fair agreement with the experiment ($\sim 0.82 \pm 0.07$ THz at 1200 K).

It is much more difficult to estimate the temperature dependence of the frequency of the H -point phonon. As mentioned earlier, the dip in the phonon dispersion curves at this point is due to the splitting of the bands about the Fermi level. There are, therefore, two additional effects which become important. The thermal disorder causes a smearing of the energy bands and reduces the effectiveness of the nesting features of the bands in producing the Kohn anomaly—thus contributing to a rise in the phonon frequency with increasing temperature.¹⁵ A second effect, which is present because of the involvement of electronic states close to the Fermi energy, is the decrease with increasing temperature of the electron-phonon renormalization of electronic states.¹³ This effect by itself would cause a decrease of the phonon frequency. Thus the temperature dependence of the H -point phonon is determined by the delicate balance among lattice expansion, thermal disorder, anharmonic effects, and the decrease of the electron-phonon renormalization. Following a similar procedure to that used for the $(\frac{2}{3}, \frac{2}{3}, \frac{2}{3})$ mode, we estimated the effect of lattice expansion (a decrease of 0.27 ± 0.03 THz) and that of anharmonicity (an increase of ~ 0.7 THz). Experimentally, the H -point frequency shows little temperature dependence from 10.5 K to room temperature and increases by approximately 0.2 THz when the temperature is increased to 1200 K. The experimentally measured frequency shift at H is of the same order of magnitude as the theoretical estimate. However, no definitive conclusion can be drawn regarding the agreement at the point H between theory and experiment, since at present there is no reliable procedure to treat the effects of thermal disorder.

ACKNOWLEDGMENTS

Ames Laboratory is operated for the U. S. Department of Energy by Iowa State University under Contract No. W-7405-Eng-82; this work was supported by the Director for Energy Research, Office of Basic Energy Sciences.

¹A. D. B. Woods and S. H. Chen, *Solid State Commun.* **2**, 233 (1964).

²B. M. Powell, P. Martel, and A. D. B. Woods, *Phys. Rev.* **171**, 727 (1968); *Can. J. Phys.* **55**, 1601 (1977).

³C. B. Walker and P. A. Egelstaff, *Phys. Rev.* **177**, 1111 (1969).

⁴S. H. Chen and B. N. Brockhouse, *Solid State Commun.* **2**, 73 (1964).

⁵H. B. Møller and A. R. Mackintosh, in *Inelastic Scattering of*

Neutrons (IAEA, Vienna, 1965), Vol. I, p. 95.

⁶W. M. Shaw and L. D. Muhlestein, *Phys. Rev. B* **4**, 969 (1971).

⁷L. D. Muhlestein, E. Gürmen, and R. M. Cunningham, in *Inelastic Scattering of Neutrons* (IAEA, Vienna, 1972), p. 53.

⁸D. L. Price, K. S. Singwi, and M. P. Tosi, *Phys. Rev. B* **2**, 2983 (1970).

⁹C. Falter, W. Ludwig, M. Selmeke, and W. Zierau, *Phys. Lett.* **90A**, 250 (1982).

- ¹⁰W. J. L. Buyers, B. M. Powell, and A. D. B. Woods, *Can. J. Phys.* **50**, 3069 (1972).
- ¹¹C. M. Varma and W. Weber, *Phys. Rev. B* **19**, 6142 (1979).
- ¹²K.-M. Ho, C. L. Fu, B. N. Harmon, W. Weber, and D. R. Hamann, *Phys. Rev. Lett.* **49**, 673 (1982) and references therein.
- ¹³K.-M. Ho, C. L. Fu, and B. N. Harmon (unpublished).
- ¹⁴D. C. Wallace, *Thermodynamics of Crystals* (Wiley, New York, 1972).
- ¹⁵The shift of the phonon frequency due to the temperature dependence of the Fermi-Dirac occupation of the electronic energy bands was evaluated and found to be insignificant.